Available online at www.eccomasproceedia.org
Eccomas Proceedia COMPDYN (2025) 466 -4674

ECCOMAS Proceedia

COMPDYN 2025
10th ECCOMAS Thematic Conference on
Computational Methods in Structural Dynamics and Earthquake Engineering
M. Papadrakakis, M. Fragiadakis (eds.)
Rhodes Island, Greece, 15-18 June 2025

DYNAMIC SOIL PRESSURES ON RIGID VERTICAL ROTATIONAL WALLS IN PRESENCE OF GENERALISED INHOMOGENEOUS SOILS

Armando Della Corte[1], Nunzia Letizia[1], Maria Giovanna Durante[2], Aggelos Tsikas[3], Adel Younan[4], Stijn François[5], and George Anoyatis[1]

[1]KU Leuven, Department of Civil Engineering, Hydraulics and Geotechnics Section
Spoorwegstraat 12, Bruges, 8200, Belgium
armando.dellacorte@kuleuven.be, nunzia.letizia@kuleuven.be, george.anoyatis@kuleuven.be

[2] University of Calabria, Department of Environmental Engineering
Via Pietro Bucci, 87036, Rende (CS), Italy
mariagiovanna.durante@unical.it

[3] Quantum Neural Technologies S.A. (QNT)
Patriarchou Ioakeim 34, Athens, 10675, Greece
ait@monogramgroup.eu

[4] Engineering Consultant
Sugar Land, Texas, United States
ahyounan@gmail.com

[5] KU Leuven, Department of Civil Engineering, Structural Mechanics Section
Kasteelpark Arenberg 40, Leuven, 3001, Belgium
stijn.francois@kuleuven.be

Abstract. *A novel benchmark semi-analytical solution is derived for the dynamic pressures and associated forces induced by ground shaking on rigid vertical walls supported on rotationally compliant footing and retaining soils with a generalised continuous variation of the soil stiffness with depth. Following the pioneering work of Veletsos and Younan in 1994 the proposed model assumes that no vertical normal stresses develop anywhere in the soil medium and that the horizontal variation of vertical displacements is negligible. This approximation reduces the two elastodynamic equations that govern the soil motion under plane strain conditions to one, that satisfies the equilibrium in the horizontal direction. The soil inhomogeneity is introduced via a power law variation of shear modulus with depth and is tackled by employing simple trigonometric functions to capture soil modes. The solution is expressed in the form of a generalised Fourier series and the effects of wall rotations on the dynamic wall pressures and associated forces are accounted for using an appropriate rocking spring at the base of the wall. The model's predictions are found to be in good agreement with finite element method simulations.*

Keywords: Dynamic Wall Pressures, Elastodynamic Model, Generalised Soil Inhomogeneity, Rotational Walls, Seismic, Earthquake.

ISSN:2623-3347 © 2025 The Authors. Published by Eccomas Proceedia.
Peer-review under responsibility of the organizing committee of COMPDYN 2025.
doi: 10.7712/120125.12766.25860

1 INTRODUCTION

During earthquake shaking, seismic pressures and the corresponding forces arise on earth-retaining structures. The evaluation of these pressures is fundamental for the analysis and design of earth-retaining structures. The methods that have been proposed to evaluate these effects can be classified into four major groups: Group A: limit-state analysis methods; Group B: Winkler-type solutions; Group C: exact and approximate analytical elastodynamic solutions; Group D: numerical solution methods, primarily finite element (FE). Methods from Group A assume that a horizontal pseudo-static seismic coefficient acts additionally on an active Coulomb-type wedge to generate a dynamic increment of the earth pressure [1–4]. Such methods overlook critical aspects of the dynamics of the problem, such as wave propagation and soil structure interaction [5]. Methods from Group B use pertinent Winkler-spring available in the literature for kinematic wall-soil interaction that generates seismic earth pressures [6–9]. Winkler-type solutions are easy to implement and can generate fast and accurate predictions (depending on selecting the appropriate Winkler springs [10]). Methods from Group C use elastodynamic theory to evaluate the system's response, assuming that the wall is not yielding and the retaining soil's response is linear elastic. In the elastodynamic solutions, the soil is treated as an (approximate) continuum rather than as a bed of independent Winkler springs uniformly distributed along the wall height, representing an alternative to Winkler formulation models. Methods from Group D are the most comprehensive and powerful technique for several reasons [11]. However such methods can be computationally expensive, especially for non-linear dynamic analyses. Elastodynamic solutions (from Group C) represent a cost-effective alternative for evaluating the seismic earth pressures and the corresponding forces. These models offer the advantage of being theoretically sound and self-standing as they do not employ empirical formulae or constants and they also avoid issues associated with mesh construction and reflections at the boundaries compared to numerical solution methods.

1.1 Available analytical solutions and proposed model

The first analytical solutions were developed by Matsuo and Ohara [12] in the 1960s. Subsequently, Wood [13] in 1973 derived an exact elastodynamic solution for a pair of rigid walls, while Scott [6] proposed a simplified Winkler model for single walls in the same year. In subsequent years, numerous approximate elastodynamic models were introduced to extend these pioneering studies. These extensions addressed more complex scenarios, such as flexible walls, rotationally constrained walls at the base, elastic bedrock, and inhomogeneous or poroelastic soils [5, 14–24]. Over time, exact solutions under plane strain conditions were also derived [11, 25–27]. While these exact solutions are powerful, they have received comparatively less attention in engineering practice, primarily due to their computational complexity and sophistication. Despite extensive research, no semi-analytical benchmark model currently exists to address dynamic pressures and associated forces on rigid rotational walls retaining a generalised inhomogeneous backfill. This study develops a novel benchmark semi-analytical elastodynamic solution for the dynamic response of rigid single rotational walls retaining soils with a generalised continuous variation of soil stiffness with depth. The proposed model builds upon the seminal work of Veletsos and Younan [16] and the recent advancements by Della Corte et al. [24] to extend the analysis to rigid rotational walls retaining generalised inhomogeneous soils. Following Veletsos and Younan [16], the equilibrium in the vertical direction is neglected by assuming that no vertical normal stresses develop anywhere in the medium and that the horizontal variation of vertical displacements is negligible. Soil inhomogeneity is introduced through a power-law variation of shear modulus with depth and is addressed using simple trigonometric functions to capture soil modes. The novelty of the proposed model lies in its ability to faithfully represent the soil modes of the inhomogeneous backfill in terms of a generalised Fourier series, expressed as a combination of familiar sinusoidal functions. The general solution is formulated in the form of a generalised Fourier series, and the effects of wall rotations on dynamic wall pressures and associated forces are incorporated through an appropriate rocking spring at the base of the wall. The model's predictions are found to be in very good agreement with finite element method simulations across a wide range of frequencies and selected soil-wall configurations.

2 MODEL DEVELOPMENT

The problem considered in this work is depicted in Figure1: a semi-infinite, non-homogeneous viscoelastic stratum of thickness H which is free at its upper surface, bonded to a rigid base, and retained along one of its vertical boundaries by a rigid rotational wall. The wall is elastically constrained against rotation at its base, the stiffness of the rotational constraint being denoted by R^*_ϑ. The wall and the base of the soil layer are excited by a space-invariant harmonic motion $\ddot{u}_{\mathrm{g}}(t)$. Elastic pressures and forces are induced on the walls by ground shaking which is induced by the passage of vertically propagating S-waves in the medium. The soil is characterized by its Poisson's ratio ν_{s}, material damping of the hysteretic type β_{s}, and mass density ρ_{s}. The gov-

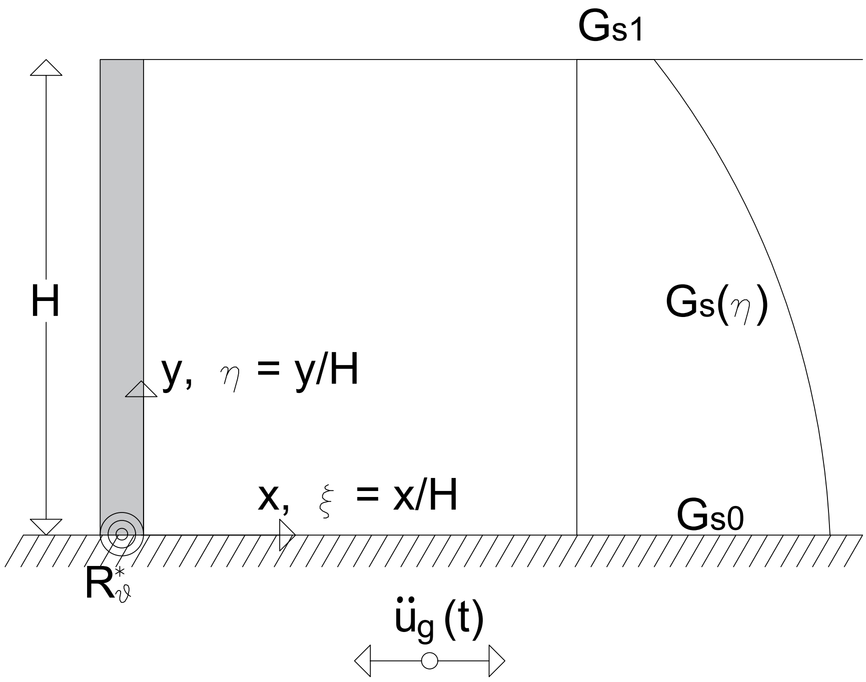

Figure 1: Problem considered: single rigid rotational wall retaining a generalised vertically inhomogeneous backfill excited by an harmonic motion $\ddot{u}_{\mathrm{g}}(t)$.

erning equation of motion in the horizontal direction of the generalised inhomogeneous backfill is [14, 16, 24]

$$\psi_0^2\, G^*_{\mathrm{s}} \frac{\partial^2 u}{\partial \xi^2} \;+\; \frac{\partial}{\partial \eta}\left(G^*_{\mathrm{s}} \frac{\partial u}{\partial \eta}\right) \;=\; \rho_{\mathrm{s}}\, H^2 \frac{\partial^2 u}{\partial t^2} \;+\; \rho_{\mathrm{s}}\, H^2\, \ddot{u}_g(t) \tag{1}$$

where $\psi_0^2 = 2/(1-\nu_{\mathrm{s}})$ is a dimensionless compressibility coefficient; $u = u(\xi,\eta)$ is the horizontal soil displacement relative to the base; and $\xi = x/H$ and $\eta = y/H$ are dimensional spatial variables. In Equation (1), $G_{\mathrm{s}}^* = G_{\mathrm{s}}^*(\eta) = G_{\mathrm{s}}(\eta)(1+2i\beta_{\mathrm{s}})$ is the complex-valued soil shear modulus, the variation of which with depth is expressed by the following power law function:

$$G_{\mathrm{s}}^*(\eta) \;=\; G_{\mathrm{s0}}^*\,\left[b+(1-b)\,(1-\eta)\right]^n \tag{2}$$

where n and b are dimensionless inhomogeneity parameters. b links the stiffness at the surface of the layer G_{s1} to the stiffness at its base G_{s0}, that is, $b = (G_{\mathrm{s1}}/G_{\mathrm{s0}})^{1/n}$. Following the work of Veletsos and Younan [16], Equation (1) is derived under the physically motivated assumptions that no dynamic vertical stresses develop anywhere in the medium and that the horizontal variation of vertical displacements is negligible. The horizontal normal stress can be written as [15]

$$\sigma_x \;=\; \psi_0^2\, G_{\mathrm{s}}^*\,\frac{1}{H}\,\frac{\partial u}{\partial \xi} \tag{3}$$

Considering harmonic input motion, the excitation at the base of the wall can be expressed as $\ddot{u}_g(t) = \ddot{u}_g\, e^{i\omega t}$, where $\ddot{u}_g$ is the excitation amplitude and ω is the circular frequency of the excitation. The horizontal soil displacement, relative to the rigid base, can be expressed as $u(\xi,\eta,t) = U(\xi,\eta,\omega)\,e^{i\omega t}$, in which $U(\xi,\eta,\omega)$ is the complex-valued soil response amplitude. $U(\xi,\eta,\omega)$ can be expressed in the form of generalised Fourier series as a linear combination of the soil modes Φ_m [15]

$$U(\xi,\eta,\omega) \;=\; \sum_{m=1}^{\infty} U_m(\xi,\omega)\,\Phi_m(\eta,\omega) \tag{4}$$

where $m = 1,2,3,...$ is a real positive integer. Substituting Equation (4) into Equation (1), applying the orthogonality identity of the soil modes, and expanding the term $\ddot{u}_{\mathrm{g}}$ in the right-hand side of Equation (1) in the form

$$\ddot{u}_{\mathrm{g}}(t) \;=\; \sum_{m=1}^{\infty} (\ddot{u}_{\mathrm{g}})_m\, G_{\mathrm{s}}^*\,\Phi_m \tag{5}$$

one obtains [24]:

$$\frac{d^2U_m}{d\xi^2} \;-\; \left(\frac{a_m}{\psi_0}\right)^2 U_m \;=\; \rho_{\mathrm{s}}\left(\frac{H}{\psi_0}\right)^2 (\ddot{u}_g)_m \tag{6}$$

where the coefficients $(\ddot{u}_{\mathrm{g}})_m$ can be obtained by applying the orthogonality identity [24]

$$(\ddot{u}_g)_m \;=\; \frac{\ddot{u}_g \int_0^1 \Phi_m\, d\eta}{\int_0^1 G_{\mathrm{s}}^* \Phi_m^2\, d\eta} \tag{7}$$

The general solution to Equation (6) is given by

$$U_m(\xi,\omega) \;=\; A_m\, e^{\left(\frac{a_m}{\psi_0}\right)\xi} + B_m\, e^{-\left(\frac{a_m}{\psi_0}\right)\xi} \;-\; \rho_{\mathrm{s}}\left(\frac{H}{a_m}\right)^2 (\ddot{u}_g)_m \tag{8}$$

in which a_m are the m-eigenvalues of the Sturm-Liouville problem, which arises from applying the method of separation of variables to Equation (1) [24]. Constant A_m in Equation (8) must vanish to ensure bounded response at distances far from the wall. Constant B_m is determined enforcing the following boundary condition $U_m(0,\eta,\omega) \ = \ \mathrm{w}(\eta,t)$; where $\mathrm{w}(\eta,t) = \theta\eta H$ is the horizontal displacement of the wall, and $\theta(t) = \Theta e^{i\omega t}$ is the wall rotation with Θ being its complex-valued amplitude [16]. The resulting expression for the horizontal soil displacement in the medium is

$$U(\xi,\eta,\omega) \ = \ \sum_{m=1}^{\infty}\left[\left(e^{-\left(\dfrac{a_m}{\psi_0}\right)\xi} - 1\right)\rho_s\left(\frac{H}{a_m}\right)^2(\ddot{u}_g)_m + \mathrm{W}_m e^{-\left(\dfrac{a_m}{\psi_0}\right)\xi}\right]\Phi_m \tag{9}$$

where W_m stands for the series coefficient which arises from expanding in series the wall displacement as $\mathrm{w}(\eta,t) = \sum_{m=1}^{\infty}\mathrm{W}_m\bar{G}_\mathrm{s}\Phi_m$ in which $\bar{G}_\mathrm{s} = G^*_{\mathrm{s}1}/G^*_{\mathrm{s}0}$ is a dimensionless soil shear modulus, and

$$\mathrm{W}_m \ = \ \frac{\Theta H\int_0^1 \eta\Phi_m\,d\eta}{\int_0^1 \bar{G}_\mathrm{s}\Phi_m^2\,d\eta} \tag{10}$$

Making use of Equations (3) and (10) the resulting expression for the dynamic wall pressure at soil-wall interface can be expressed as

$$\sigma_{\mathrm{x},0}(\eta,\omega) \ = \ -\sum_{m=1}^{\infty}\psi_0 G^*_s\left[\rho_s\frac{H}{a_m}(\ddot{u}_g)_m \ + \ a_m\frac{\Theta\int_0^1\eta\Phi_m\,d\eta}{\int_0^1\bar{G}_\mathrm{s}\Phi_m^2\,d\eta}\right]\Phi_m \tag{11}$$

The unknown rotation amplitude Θ in the Equation (11) is determined by satisfying the equilibrium of moments about the wall base [16]. The amplitude of the base shear $Q_\mathrm{b}(\omega)$ and base moment $M_\mathrm{b}(\omega)$ can be expressed by integrating along the wall height the horizontal stresses given from Equation (11):

$$Q_\mathrm{b}(\omega) \ = \ H\int_0^1 \sigma_{\mathrm{x},0}(\eta,\omega)\,d\eta \tag{12}$$

and

$$M_\mathrm{b}(\omega) \ = \ H^2\int_0^1 \sigma_{\mathrm{x},0}(\eta,\omega)\eta\,d\eta \tag{13}$$

In addition to the parameters governing the response of the system with the fixed-based wall, the dynamic response of the elastically constrained wall depends on the relative measure of the relative flexibilities of the wall and the medium [16].

$$d_\theta \ = \ \frac{G^*_{\mathrm{s}0}H^2}{R^*_\theta} \tag{14}$$

2.1 Soil Modes

The soil modes $\Phi_m = \Phi_m(\eta,\omega)$ should satisfy the Sturm–Liouville equation, which arises from applying the method of separation of variables to Equation (1) [24]. The Sturm–Liouville equation is solved by expressing the soil modes $\Phi = \Phi_m(z,\omega)$ in terms of Fourier series as:

$$\Phi_m \ = \ \sum_{k=1}^{\infty} S_k^m\,\Psi_k \tag{15}$$

and enforcing the following boundary conditions

$$\Phi_m(0,\omega) \;=\; 0, \quad \text{and} \quad \left.\frac{d\Phi_m}{d\eta}\right|_{\eta=1,\omega} \;=\; 0 \tag{16}$$

In Equation (15) $S_k^m(\omega)$ are the Fourier coefficients to be determined, and $\Psi_k(z)$ are sinusoidal functions of the form $\sin(\alpha_k z)$ where $\alpha_k = (\pi/2H)(2j-1)$ in which $k = 1,\, 2,\, 3,\, \dots N$. Using Equation (15), making use of the orthogonality property of the trigonometric functions and integrating along the thickness of the soil layer, the Sturm–Liouville problem can be expressed as:

$$\sum_{k=1}^{\infty} S_k^m \int_0^1 G_{\mathrm{s}}^* \, Y_m' \, Y_k' \, d\eta \;-\; \omega^2 \, \rho_{\mathrm{s}} \, H^2 \, S_m \int_0^1 Y_k^2 \, d\eta \;-\; \sum_{k=1}^{\infty} S_k^m \, a_m^2 \int_0^1 G_{\mathrm{s}}^* \, Y_m \, Y_k \, d\eta \;=\; 0 \tag{17}$$

The eigenvalues, α_m, and the coefficients, S_k^m, are frequency dependent and can be obtained by solving a $k \times m$ system of algebraic equations that emerges from Equation (17), at a given frequency [24].

3 MODEL VERIFICATION AND NUMERICAL RESULTS

3.1 Finite element model

Numerical analyses were conducted using the commercial finite-element software ABAQUS [28]. The problem of a retaining wall investigated in this study can be modelled assuming plane-strain conditions, thus defining a two-dimensional numerical model. A section of the mesh of the finite element model of the wall-soil system is shown in Figure 2. The wall is modelled as a

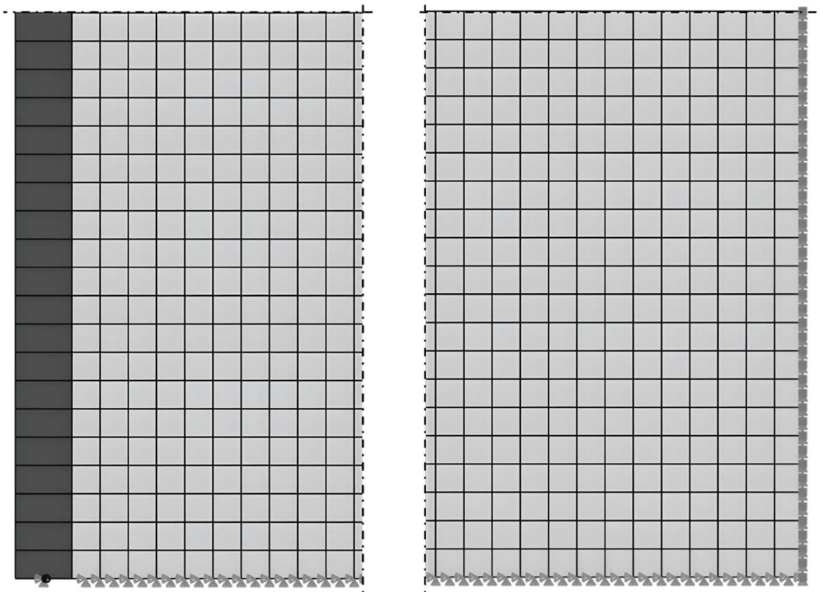

Figure 2: Finite-element discretization of the wall-soil system in Abaqus.

rigid body of height $H = 8\,\mathrm{m}$. The soil is modelled as an elastic material, characterized by its density $\rho_{\mathrm{s}} = 1.8\,\mathrm{T/m^3}$, Poisson's ratio $\nu_{\mathrm{s}} = 1/3$, and hysteretic material damping $\beta_{\mathrm{s}} = 0.05$. For the analyses of a homogeneous backfill, the propagation velocity of the shear waves V_{s} in the soil was set equal to $100\,\mathrm{m/s}$, such that the soil shear modulus results being $18\,\mathrm{MPa}$.

The model size and mesh properties were derived from a sensitivity analysis performed to guarantee the accuracy of the numerical results. Accordingly, in order to prevent the lateral boundary of the model from affecting the observed response, the model extends $50\,H$ horizontally, from the wall. To prevent reflections from the horizontal surface of the soil model, horizontal and vertical dashpots were used at the vertical free boundary, to absorb the energy from P and S waves, respectively. The model was discretised using eight-node square quadrilateral, plane-strain elements (CPE8), with size equal to $0.1\,\mathrm{m}$. The soil-wall interface was assumed fully-bonded, to conduct a first comparative study with the analytical results. The excitation was introduced by prescribed horizontal displacements at the nodes at the base of the wall and the soil, using a direct-solution, steady-state dynamic analysis, which provides a steady-state amplitude and phase of the system's response at a given excitation frequency. To model the bedrock, the nodes along the bottom boundary of the soil model were restrained against displacements and rotation. On the other hand, the wall was elastically constrained against rotation by introducing a rotational spring at its base characterized by stiffness R_θ^*.

3.2 Numerical results

Figure 3 shows the distribution of the real part of the horizontal pressure for a rotationally constrained wall retaining a homogeneous backfill for static excitation frequency ($\omega \approx 0$). Results from the original model of Veletsos and Younan [16], finite element (FE) analyses, and the proposed solution are compared for two selected rocking flexibility factors: $d_\theta = 1$ (Figure 3a) and $d_\theta = 5$ (Figure 3b). $N = 500$ modes have been used in the analysis, with Poisson's ratio $\nu_\mathrm{s} = 1/3$, soil material damping $\beta_\mathrm{s} = 0.05$. The wall is assumed to be massless in the following figures. The proposed solution exhibits excellent agreement with both Veletsos and Younan's

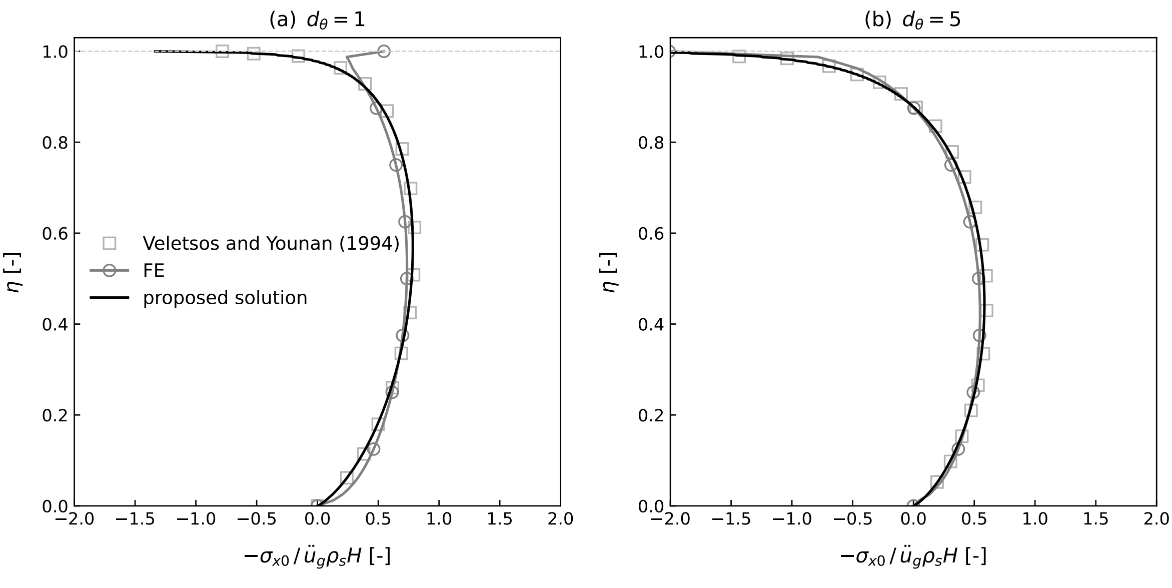

Figure 3: Comparison of the proposed solution against Veletsos and Younan's model [16] and finite element (FE) results for the real part of normalised horizontal pressure on a rotationally constrained wall retaining a homogeneous backfill for two selected values of rocking flexibility: (a) $d_\theta = 1$ and (b) $d_\theta = 5$; $\nu_\mathrm{s} = 1/3$, $N = 500$, $\omega \approx 0$.

model [16] and FE results, validating its applicability to homogeneous backfill conditions. It

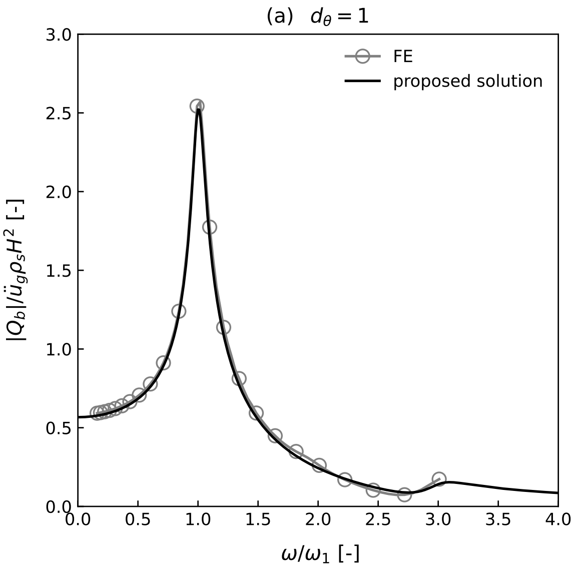

Figure 4: Comparison of the proposed solution against finite element (FE) analyses for normalised base shear on a rotationally constrained wall retaining a homogeneous backfill for two selected values of rocking flexibility: (a) $d_\theta = 1$ and (b) $d_\theta = 5$; $\nu_s = 1/3$, $\beta_s = 0.05$, $N = 25$.

can be seen that wall flexibility introduces a singularity at the top of the wall [16]. The variation of the amplitude of the normalised base shear $|Q_b|$ with normalised excitation frequency ω/ω_1 is plotted in Figure 4 for a homogeneous backfill. The agreement of the proposed solution with FE results is excellent over the entire frequency range and for both rocking flexibility factors (Figures 4a and 4b), confirming the predictive power of the proposed solution. As expected, the base shear, pressures and base moments decrease with increasing wall flexibility (larger values of d_θ). Figure 5 presents the variation of the normalized base shear amplitude, $|Q_b|$, with the normalized excitation frequency, ω/ω_1, for two cases: a fixed-based, irrotational wall ($d_\theta = 0$) and a rotationally rigid wall ($d_\theta = 1$). The results are provided for both a homogeneous backfill (Figure 5a) and a backfill with a parabolic variation of the shear modulus with depth (Figure 5b). For comparison, finite element (FE) results for the rotationally constrained wall ($d_\theta = 1$) are also included. The comparison with FE results shows overall very good agreement. For the inhomogeneous case (Figure 5b, $d_\theta = 1$), the agreement between the proposed solution and FE results is slightly less accurate than for the homogeneous case. The proposed solution slightly underestimates the base shear across the entire frequency range, except at resonance, where it slightly overestimates it. Notably, the reduction in base shear due to wall flexibility is not uniform across all frequencies, particularly in the presence of an inhomogeneous backfill. Furthermore, soil inhomogeneity leads to an overall reduction in base shear compared to the homogeneous case, with this effect being less pronounced for rotationally constrained walls.

4 CONCLUSIONS

A novel benchmark semi-analytical solution is derived for the dynamic pressures and associated forces induced by ground shaking on rigid vertical walls supported on rotationally compliant footing and retaining soils with a generalised continuous variation of the soil stiffness with depth, extending the seminal work of Veletsos and Younan [16]. The proposed model assumes that no vertical normal stresses develop anywhere in the soil medium and that the horizontal variation of vertical displacements is negligible. This approximation reduces

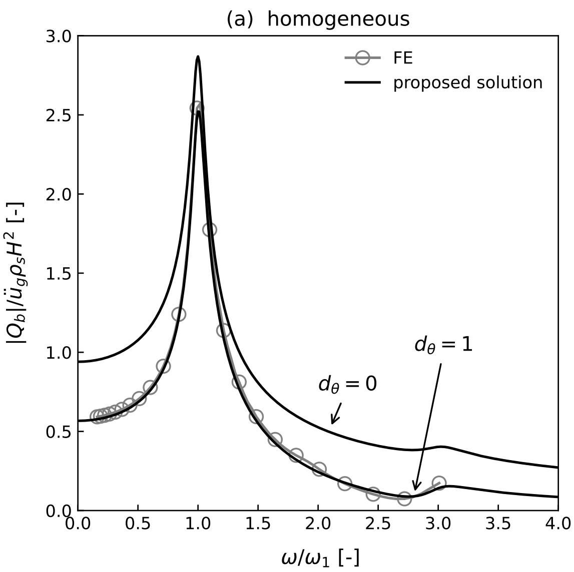

Figure 5: Comparison of the proposed solution against finite element (FE) analyses for normalised base shear on a rotationally constrained wall retaining a homogeneous backfill (a) and an inhomogeneous backfill (b); $d_\theta = 1$, $\nu_s = 1/3$, $\beta_s = 0.05$, $N = 25$, $n = 0.5$, $G_{s1}/G_{s0} = 0.25$.

the two elastodynamic equations that govern the soil motion under plane strain conditions to one, which satisfies the equilibrium in the horizontal direction. To validate the model, the analysis of a homogeneous backfill is first revisited, showing excellent agreement with both Veletsos and Younan's solution [16] and finite element (FE) results, confirming its applicability to homogeneous backfill conditions. Soil inhomogeneity affects the system's response, leading to an overall reduction in base shear compared to the homogeneous case, with this effect being less pronounced for rotationally constrained walls. Furthermore, the reduction in base shear due to wall flexibility is not uniform across all frequencies, particularly in the presence of an inhomogeneous backfill. Future research endeavours will focus on expanding the model to encompass the broader applications of flexible wall and the more complex nonlinear scenario through linear equivalent analyses. As a final remark, to ensure results from this research can be verified and reproduced, python scripts and data are shared on a KU Leuven web page titled Soil–Structure Interaction Toolkit, which can be accessed following the link `https://bwk.kuleuven.be/projects/SSItk/` (upon acceptance of the manuscript). This study aims to promote open science and enhance collaboration and innovation in the field. Open access to these resources can facilitate reproducibility and verification of results, and further encourage continuous improvement and adaptation of solutions.

ACKNOWLEDGEMENTS

The research proposed in this paper was supported by the Deep Foundations Institute (DFI) through DFI Committee Project Fund scheme, and the project titled "DRWSI Dynamic Retaining Wall-Soil Interaction: New Developments and Web-platform" (CPF-2022-SSMC-1). The authors are grateful to DFI for this support.

REFERENCES

[1] C. A. Coulomb, *Essai sur une application des règles de maximis et minimis à quelques problèmes de statique, relatifs à l'architecture*. Paris: Académie Royale des Sciences, 1776.

[2] S. Okabe, General theory on earth pressure and seismic stability of retaining wall and dam. *Journal of Japan Society of Civil Engineers*, 10(6), 1277–1323, 1924.

[3] N. Mononobe, On the determination of earth pressure during earthquakes. In *Proceedings of the World Engineering Congress*, vol. 9, 177–185, 1929. https://cir.nii.ac.jp/crid/1570009750030450560.

[4] G. Mylonakis, P. Kloukinas, and C. Papantonopoulos, An alternative to the Mononobe–Okabe equations for seismic earth pressures. *Soil Dynamics and Earthquake Engineering*, 27(10), 957–969, 2007. https://doi.org/10.1016/j.soildyn.2007.01.004.

[5] S. J. Brandenberg, G. Mylonakis, and J. P. Stewart, Approximate solution for seismic earth pressures on rigid walls retaining inhomogeneous elastic soil. *Soil Dynamics and Earthquake Engineering*, 97, 468–477, 2017. https://doi.org/10.1016/j.soildyn.2017.03.028.

[6] R. F. Scott, Earthquake-induced earth pressure on retaining walls. In *Proceedings of the 5th World Conference on Earthquake Engineering*, Rome, Italy: Elsevier, 1973, pp. 1611–1620. https://www.nicee.org/wcee/search5.php.

[7] S. J. Brandenberg, G. Mylonakis, and J. P. Stewart, Kinematic framework for evaluating seismic earth pressures on retaining walls. *Journal of Geotechnical and Geoenvironmental Engineering*, 141(7), 04015031, 2015. https://doi.org/10.1061/(ASCE)GT.1943-5606.0001312.

[8] S. J. Brandenberg, M. G. Durante, G. Mylonakis, and J. P. Stewart, Winkler solution for seismic earth pressures exerted on flexible walls by vertically inhomogeneous soil. *Journal of Geotechnical and Geoenvironmental Engineering*, 146(11), 04020127, 2020. https://doi.org/10.1061/(ASCE)GT.1943-5606.0002374.

[9] M. G. Durante, J. P. Stewart, S. J. Brandenberg, and G. Mylonakis, Simplified solution for seismic earth pressures exerted on flexible walls. *Earthquake Spectra*, 38(3), 1872–1892, 2022. https://doi.org/10.1177/87552930221083326.

[10] G. Anoyatis and A. Lemnitzer, Kinematic Winkler modulus for laterally-loaded piles. *Soils and Foundations*, 57(3), 453–471, 2017. https://doi.org/10.1016/j.sandf.2017.05.011.

[11] G. Degrande, E. Praet, B. Van Zegbroeck, and P. Van Marcke, Dynamic interaction between the soil and an anchored sheet pile during seismic excitation. *International Journal for Numerical and Analytical Methods in Geomechanics*, 26(6), 605–631, 2002. https://doi.org/10.1002/nag.214.

[12] H. Matsuo and S. Ohara, Lateral earth pressure and stability of quay walls during earthquakes. In *Proceedings of the 2nd World Conference on Earthquake Engineering*, vol. 1, Tokyo, Japan: JSCE, 1960, pp. 165–181. https://www.nicee.org/wcee/search2.php.

[13] J. H. Wood, Earthquake-induced soil pressures on structures. Ph.D. Dissertation, California Institute of Technology, 1973. https://doi.org/10.7907/MZWQ-BA46, https://resolver.caltech.edu/CaltechThesis:10152019-101037996.

[14] R. A. Arias, F. J. Sanchez-Sesma, and E. Ovando-Shelley, A simplified elastic model for seismic analysis of earth-retaining structures with limited displacements. In *Proceedings of the 1st International Conference on Recent Advances in Geotechnical Earthquake Engineering and Soil Dynamics*, 26 April – 3 May, Missouri, U.S.A., 1981.

[15] A. S. Veletsos and A. H. Younan, Dynamic soil pressures on rigid vertical walls. *Earthquake Engineering & Structural Dynamics*, 23(3), 275–301, 1994. https://doi.org/10.1002/eqe.4290230305.

[16] A. S. Veletsos and A. H. Younan, Dynamic modeling and response of soil-wall systems. *Journal of Geotechnical Engineering*, 120(12), 2155–2179, 1994. https://doi.org/10.1061/(ASCE)0733-9410(1994)120:12(2155).

[17] A. S. Veletsos, V. H. Parikh, and A. H. Younan, Dynamic response of a pair of walls retaining a viscoelastic solid. *Earthquake Engineering & Structural Dynamics*, 24(12), 1567–1589, 1995. https://doi.org/10.1002/eqe.4290241203.

[18] A. S. Veletsos and A. H. Younan, Dynamic response of cantilever retaining walls. *Journal of Geotechnical Engineering*, Proceedings of the ASCE, 123(2), 161–172, 1997. https://doi.org/10.1061/(ASCE)1090-0241(1997)123:2(161).

[19] X. Li, Dynamic analysis of rigid walls considering flexible foundation. *Journal of Geotechnical and Geoenvironmental Engineering*, 125(9), 803–806, 1999. https://doi.org/10.1061/(ASCE)1090-0241(1999)125:9(803).

[20] A. H. Younan and A. S. Veletsos, Dynamic response of flexible retaining walls. *Earthquake Engineering & Structural Dynamics*, 29(12), 1815–1844, 2000. https://doi.org/10.1002/1096-9845(200012)29:121815::AID-EQE9933.0.CO;2-Z.

[21] D. D. Theodorakopoulos, P. E. Chassiakos, and D. E. Beskos, Dynamic pressures on rigid cantilever walls retaining poroelastic soil media. Part I. First method of solution. *Soil Dynamics and Earthquake Engineering*, 21(1), 315–338, 2001. https://doi.org/10.1016/S0267-7261(01)00009-4.

[22] P. Kloukinas, M. Langousis, and G. Mylonakis, Simple wave solution for seismic earth pressures on nonyielding walls. *Journal of Geotechnical and Geoenvironmental Engineering*, 138(12), 1514–1519, 2012. https://doi.org/10.1061/(ASCE)GT.1943-5606.0000721.

[23] G. Anoyatis, S. François, N. Letizia, A. Della Corte, O. Orakci, and A. Tsikas, Seismic soil pressures on rigid walls retaining inhomogeneous backfills. In *Proceedings of the 18th World Conference on Earthquake Engineering (WCEE 2024)*, Milan, Italy: Springer, 2024. Session ID: GEO-3 Title GEOTECHNICAL SEISMIC ISOLATION (GSI), Convenors: H.-H. Tsang, L. Montrasio, D. Pitilakis.

[24] A. Della Corte, N. Letizia, A. Tsikas, S. François, and G. Anoyatis, Dynamic soil pressures on rigid vertical walls in presence of generalized inhomogeneous soils. *Earthquake Engineering and Structural Dynamics*, 2025, (accepted).

[25] G. Papazafeiropoulos and P. N. Psarropoulos, "Analytical Evaluation of the Dynamic Distress of Rigid Fixed-Base Retaining Systems," *Soil Dynamics and Earthquake Engineering*, **30**, no. 12 (2010): 1446–1461, `https://doi.org/10.1016/j.soildyn.2010.05.004`.

[26] G. A. Papagiannopoulos, D. E. Beskos, and T. Triantafyllidis, Seismic pressures on rigid cantilever walls retaining linear poroelastic soil: An exact solution. *Soil Dynamics and Earthquake Engineering*, 77(10), 208–219, 2015. `https://doi.org/10.1016/j.soildyn.2015.05.015`.

[27] C. Vrettos, D. Beskos, and T. Triantafyllidis, "Seismic Pressures on Rigid Cantilever Walls Retaining Elastic Continuously Nonhomogeneous Soil: An Exact Solution," *Soil Dynamics and Earthquake Engineering*, **82** (2016): 142–153, `https://doi.org/10.1016/j.soildyn.2015.12.006`.

[28] Systemes Dassault, *ABAQUS/Standard User's Manual*. Dassault Systèmes Simulia Corp, United States, 2022.